THE JOURNAL OF BIOLOGICAL CHEMISTRY VOL. 290, NO. 43, pp. 25997–26006, October 23, 2015
Published in the U.S.A.

Hepatic Insulin Resistance Following Chronic Activation of the CREB Coactivator CRTC2*

Received for publication, July 16, 2015, and in revised form, August 27, 2015 Published, JBC Papers in Press, September 4, 2015, DOI 10.1074/jbc.M115.679266

Meghan F. Hogan[‡§], Kim Ravnskjaer[‡¶], Shigenobu Matsumura[‡‖], Mark O. Huising[‡], Rebecca L. Hull[§], Steven E. Kahn[§], and Marc Montminy[‡1]**

*From the [‡]Peptide Biology Laboratories, Salk Institute for Biological Studies, La Jolla, California 92037, [§]Division of Metabolism, Endocrinology, and Nutrition, Department of Medicine, VA Puget Sound Health Care System and University of Washington, Seattle, Washington 98108, [¶]Department of Biochemistry and Molecular Biology, University of Southern Denmark, Odense, Denmark, [‖]Division of Food Science and Biotechnology, Graduate School of Agriculture, Kyoto University, Oiwake-cho, Kitashirakawa, Sakyo-ku, Kyoto, 606-8502, Japan, and **Department of Physiology and Membrane Biology, School of Medicine, University of California, Davis, California 95616*

Background: Loss of CRTC2 improves insulin sensitivity, but it is unknown if chronic CRTC2 activity causes hepatic insulin resistance.
Results: Liver expression of constitutively active CRTC2 increased hepatic glucose production, despite compensatory increases in FOXO1 phosphorylation.
Conclusion: Persistent increases in CRTC2 activation promote hepatic insulin resistance.
Significance: Disrupting CREB signaling in liver could provide therapeutic benefit against insulin resistance.

Under fasting conditions, increases in circulating concentrations of glucagon maintain glucose homeostasis via the induction of hepatic gluconeogenesis. Triggering of the cAMP pathway in hepatocytes stimulates the gluconeogenic program via the PKA-mediated phosphorylation of CREB and dephosphorylation of the cAMP-regulated CREB coactivators CRTC2 and CRTC3. In parallel, decreases in circulating insulin also increase gluconeogenic gene expression via the de-phosphorylation and activation of the forkhead transcription factor FOXO1. Hepatic gluconeogenesis is increased in insulin resistance where it contributes to the attendant hyperglycemia. Whether selective activation of the hepatic CREB/CRTC pathway is sufficient to trigger metabolic changes in other tissues is unclear, however. Modest hepatic expression of a phosphorylation-defective and therefore constitutively active CRTC2S$_{171,275}$A protein increased gluconeogenic gene expression under fasting as well as feeding conditions. Circulating glucose concentrations were constitutively elevated in CRTC2S$_{171,275}$A-expressing mice, leading to compensatory increases in circulating insulin concentrations that enhance FOXO1 phosphorylation. Despite accompanying decreases in FOXO1 activity, hepatic gluconeogenic gene expression remained elevated in CRTC2S$_{171,275}$A mice, demonstrating that chronic increases in CRTC2 activity in the liver are indeed sufficient to promote hepatic insulin resistance and to disrupt glucose homeostasis.

In unaffected and appropriately regulated systems, blood glucose levels remain remarkably constant, despite alternating periods of caloric abundance and scarcity. This level of control is preserved by balancing hepatic glucose production (gluconeogenesis and glycogenolysis) during fasting with the glucose uptake into peripheral tissues during feeding. The transition from a high-risk state to type 2 diabetes is marked by insulin resistance, and an inability for insulin to inhibit hepatic gluconeogenesis, resulting in elevated fasting blood glucose (1–4).

Under fasting conditions, increases in glucagon upregulate the gluconeogenic program by triggering the cAMP pathway (5) and stimulating the protein kinase A (PKA)[2]-mediated phosphorylation of cAMP response element-binding protein (CREB). Serine 133 phosphorylation of CREB in turn promotes recruitment of the histone acetyltransferase paralogs CREB-binding protein (CBP) and P300 (6, 7).

Superimposed on effects of the CREB:CBP pathway, cAMP also stimulates hepatic gene expression in the liver via the induction of the cAMP-regulated CREB Coactivators (CRTCs). Under basal conditions, CRTCs are phosphorylated by salt-inducible kinases (SIKs) and sequestered in the cytoplasm by association with 14-3-3 proteins (8). Triggering of the cAMP pathway promotes the inhibitory phosphorylation of salt inducible kinases (SIKs) by PKA, leading to the dephosphorylation and translocation of CRTCs to the nucleus, where they associate with relevant target genes via an interaction with CREB (8–13).

The importance of the CREB:CRTC pathway in hepatic gluconeogenesis is supported by studies in which acute RNAi-me-

* This work was supported by National Institutes of Health Grants R37DK083834 (to M. M., M. F. H.); 5T32GM007240 (to M. F. H.); 5R01DK088082 (to R. L. H.); The Clayton Foundation for Medical Research (to M. M.), the Kieckhefer Foundation (to M. M.), the Leona M. and Harry B. Helmsley Charitable Trust Grant #2012-PG-MED002 (to M. M., M. F. H.); and the Department of Veterans Affairs (S. E. K.). The authors declare that they have no conflicts of interest with the contents of this article.

[1] To whom correspondence should be addressed: Peptide Biology Laboratories, Salk Institute for Biological Studies, 10010 N. Torrey Pines Rd., La Jolla, CA 92037. Tel.: 858-453-4100 x1350; Fax: 858-552-1546; E-mail: montminy@salk.edu.

[2] The abbreviations used are: PKA, protein kinase A; CBP, CREB-binding protein; CREB, cAMP response element-binding protein; CRTC, CREB-regulated transcription coactivator; FOXO1, forkhead box protein O1; G6Pase, glucose-6-phosphatase; P300, E1A-binding protein p300; PCK1, phosphoenolpyruvate carboxykinase 1; SIK, salt inducible kinases; STZ, streptozotocin.

diated knockdown of CRTC2 in liver decreases gluconeogenic gene expression as well as circulating glucose concentrations (9, 14). Cultured hepatocytes from CRTC2 knock-out mice also exhibit decreases in glucose production (12, 15), although these effects are more modest due to compensation by CRTC3 (16).

Recognizing the importance of the CREB/CRTC2 pathway in the fasting adaptation, we wondered whether modest expression of an active form of CRTC2 in the liver would be sufficient to increase hepatic gluconeogenesis and promote insulin resistance in peripheral tissues.

We found that selective expression of a constitutively active form of CRTC2 in liver for a period of up to 5 weeks increases the set point for circulating concentrations of glucose. This stable rise in blood glucose levels promotes compensatory increases in pancreatic islet mass and insulin secretion. The results point to an important role for hepatic CRTC2 in glucose homeostasis and in the development of hepatic insulin resistance.

Experimental Procedures

Adeno-associated Viruses (AAV) Strains and Propagation—Viruses were derived from pENN AAV TBG PI (an adeno-associated virus, serotype 8 with a TBG promoter), a generous gift from Dr. Morris Birnbaum at the University of Pennsylvania. Briefly, pENN AAV TBG PI was digested with enzymes Acc65I and SalI (New England Biolabs, Danvers, MA; #R0599 and #R0138). Meanwhile, a pcDNA3 construct expressing a FLAG-tagged mouse CRTC2 with mutations S171A and S275A was amplified by PCR (primers: GCCGGTACCATGACCATGGATTACAAGGAT, and GCCGTCGACTAGGTGACACTATAGAATAGG) and then digested with Acc65I and SalI. The digested pENN AAV TBG PI was ligated with the FLAG.CRTC2AA PCR fragment and transformed in recombination-deficient *Escherichia coli* SURE cells (Agilent, Santa Clara, CA; #200238).

The resulting vectors (pENN AAV TBG PI and pENN AAV TBG PI CRTC2AA) were amplified in the Salk Institute Gene Transfer Targeting and Therapeutics Core. The amplified viruses are hereafter referred to as AAV.Empty and AAV.CRTC2AA.

Animals—Mice were housed in colony cages in a temperature controlled environment under a 12 h light/dark cycle with free access to water and a standard Chow diet (Lab Diet 5001). ChIP studies were performed using 8–10-week-old C57BL/6J mice from Jackson Laboratories (Bar Harbor, ME; <000664>). Unless noted, other studies were performed using 8–12-week-old B6(Cg)-Tyr^{c-2J}/J mice from Jackson Laboratories (<000058>). CRE-Luciferase mice were described previously (17).

Mice received daily IP injections of 75 mg streptozotocin (STZ)/kg body weight in a sodium citrate buffer for three consecutive days; controls receive buffer-only injections. Experiments were performed after 14 days after the initial injection.

Mice were injected retro-orbitally at 8–10 weeks with 10^{11} genomic copies (gc) of AAV.Empty or AAV.CRTC2AA virus as described (18, 19). All mouse experiments were performed in accordance with the Salk Institute Institutional Animal Care and Use Committee.

Mouse Genotyping—Mouse genotypes for CRE-Luciferase were determined on tail biopsies using real-time PCR with specific probes designed for luciferase (Transnetyx, Cordova, TN).

In Vivo Analysis—Pyruvate tolerance was tested in 16-hour fasted conscious mice after a baseline tail blood glucose measurement, with an intraperitoneal injection of sodium pyruvate (2 g/kg body weight) followed by tail blood glucose measurements every 15–30 min for 2 h (12).

Whole body insulin sensitivity was measured using the insulin tolerance test (ITT). For this, an intraperitoneal injection of 1 unit of insulin (Humulin-R, Eli Lilly, Indianapolis, IN)/kg body weight was administered followed by tail blood glucose measurements every 15 min for 1 h. Muscle and adipose tissue specimens for determination of Akt phosphorylation (as a measure of insulin action), mice were fasted for 4 h and then administered an intraperitoneal injection of 1 unit of insulin/kg body weight as above, and sacrificed 10 min postinjection.

For determination of fasting blood glucose levels, mice were fasted overnight for 16 h with free access to water. Refed blood glucose values were determined after 4 h of free access to food. Glucose tolerance was measured by an intraperitoneal glucose tolerance test (IPGTT). Glucose (1 g/kg, ip) was administered followed by tail blood glucose measurements every 30 min for two hours. Continuous glucose monitoring was performed as previously described (20). Briefly, the sensor (Dexcom7 system, Dexcom, San Diego, CA) was inserted under the skin in anesthetized mice and calibrated twice daily based on blood glucose values determined with a LifeScan One Touch Ultra glucometer (Chesterbrook, PA).

For *in vivo* imaging of whole body luciferase activity, fasted and fed CRE-luciferase mice were anesthetized, treated with D-luciferin (150 mg/kg, IP) and underwent intra-vital imaging in an IVIS-100 instrument (Caliper Life Sciences) as previously described (17).

Tail blood glucose values were determined using a LifeScan One Touch Ultra glucometer. Serum insulin levels were measured using the Crystal Chem Ultra Sensitive Mouse Insulin ELISA (Downers Grove, IL; #90080).

Cell Culture and in Vitro Analysis—Primary hepatocytes were derived from B6(Cg)-Tyr^{c-2J}/J or CRE-Luc mice as previously described (18, 21). Hepatocytes expressing AAV.Empty or AAV.CRTC2AA were harvested from 8–10-week-old mice infected 3 days previously with AAV, and maintained in serum-free Medium 199 (Corning, Manassas, VA; #10-060). Hepatocytes were either stimulated with glucagon (100 nmol/liter, Sigma-Aldrich #G2044) or PBS as a negative control.

Gene Expression Analysis—Total cellular RNA from whole tissue or from primary hepatocytes was extracted using the RNeasy kit (Qiagen, Valencia, CA; #74104), and cDNA was generated using the iScript select system (Bio-Rad #170-8840). cDNA was quantified via the LightCycler 480 instrument and 2× SYBR Green (Roche, Indianapolis, IA). Gene expression data are presented relative to parallel measured expression of housekeeping cDNA, for example *RPL32* (*L32*).

Protein Analysis—Total protein from whole tissue or primary hepatocytes was extracted in RIPA buffer (50 mM TRIS pH 7.5; 150 mM sodium chloride; 1 mM EDTA; 50 mM sodium fluoride; 5 mM sodium pyrophosphate; 10 mM β-glycerophosphate; 1%

Nonidet P-40) containing 1 mM sodium orthovanadate; 1 mM dithiothreitol; 2 mM phenylmethanesulfonyl fluoride; 0.25% DOC (sodium deoxycholate); and 0.1% sodium dodecyl sulfate from Sigma. Proteins were quantified using the Bio-Rad Protein Assay Kit and separated using SDS-PAGE.

Immunoprecipitation—To 1 mg of tissue lysates (1 μg/μl) was added 40 μl of pre-cleared FLAG-M2 monoclonal antibody beads (Sigma #F3165); samples were incubated with rotation overnight at 4 °C. The supernatant was removed, and beads were washed five times with lysis buffer, eluted with 2× SDS loading buffer and analyzed via Western blot.

ChIP Assays—Livers were excised and immediately cross-linked in 1% formaldehyde while being shredded. Excessive formaldehyde was inactivated with glycine after 10 min of cross-linking. Using a hypotonic lysis buffer, nuclei were isolated and homogenized with a Dounce homogenizer. Resulting chromatin was sonicated 8 times for 10 s at 50% output, precleared and incubated with the indicated antibodies overnight in the presence of phosphatase, protease, and HDAC inhibitors. Precipitated chromatin was purified, quantified by PCR (Lightcycler 480; Roche), and presented as a percentage of input chromatin as previously described (16).

Antibodies and Western Blots—Antibodies used for immunoblotting and immunofluorescence were: FLAG-M2 (1:1000, Sigma #F1804), glucagon (1:500, Sigma #G2645), histone H3 (Abcam #ab1791), Hsp90 (1:3000, SCBt #33755), insulin (1:500, Xymed #180067), pLKB1 (1:1000, Cell Signaling Technology #C6783), pFOXO1 Ser-256 (1:1000, Cell Signaling Technology #9461). For CRTC2 (1:5000), CREB (1:5000), and pCREB (1:5000), rabbit polyclonal antibodies were raised against respective antigens (Salk Institute). For all Western blots, secondary antisera were HRP-conjugated goat anti rabbit IgGs (1:5000, Bio-Rad #170-6515). Following SDS-Page, proteins were transferred to PVDF membranes (Millipore, Billerica, MA; #IPVH00010), blocked with 5% milk TBS-T followed by incubation with primary and secondary antisera. Antibody binding was visualized by HyGlo ECL (Denville, South Plainfield, NJ; #E2500).

Immunofluorescence—Live hepatocytes were plated in glass chamber slides (BD #354114), and treated as indicated. Slides were then fixed for 10 min in 4% paraformaldehyde in PBS, and blocked for 30 min [PBS with 1% donkey serum (JAX #017–000-001) and 1% BSA (Millipore #81-066-4)]. Primary antibodies were incubated overnight in PBS, and secondary antibodies linked with Alexa-Fluor-488 (donkey antigoat) or -568 (goat antiguinea pig and donkey antirabbit) (Life Technologies) were incubated for 2 h and sections were counterstained with DAPI (1:500, Invitrogen #D3571). Slides were then mounted with 70% glycerol and PBS, and images taken using a Confocal Zeiss 780. Tissues were dissected from mice and fixed in Z-Fix for 4 h, and then sectioned in 5–10 micron slices. Slides were deparaffinized and rehydrated, and antigen retrieval via citrate unmasking by boiling slides in 10 mM sodium citrate buffer, pH 6, and left at sub-boiling temperatures for 10 min, and cooled for 30 min. Slides were blocked in blocking buffer (PBS with 1% donkey serum and 1% BSA), and then incubated overnight with primary antibodies; followed by fluorescent secondary antibodies for 1 h, and counterstained DAPI. Sections were mounted with 70% glycerol and analyzed as above.

Islet Quantification—A single investigator (MFH) was blinded to viral infection for each sample and carried out histological assessment of islets. An average of 17 islets per animal was analyzed. β-cell area (percent of islet area occupied by insulin positive immunoreactivity) was computed using Image Pro Plus (Media Cybernetics, Bethesda, MD) by determining the insulin-positive areas within each islet cross-section (22), and similar calculations were performed for α cell area by determining the glucagon-positive areas within the islet.

Statistical Analysis—Data are presented as mean ± S.E. Statistical differences for one factor between two groups were determined by use of an unpaired Student's *t* test. *p* values of <0.05 were considered to be statistically significant.

Results

Acute Loss of Insulin Signaling Up-regulates CREB and CRTC2 Activities—CREB and CRTC2 are activated during fasting where they stimulate gluconeogenic gene expression following their recruitment to the promoter (Fig. 1). The CREB/CRTC2 pathway is inactivated during refeeding, leading to dismissal of CRTC2 from gluconeogenic promoters. We used the β cell toxin streptozotocin (STZ) to test the importance of insulin in regulating hepatic CREB/CRTC2 activity. Amounts of phosphorylated CREB were comparable between WT and STZ mice during fasting. By contrast with the refeeding-associated decrease in phospho-CREB amounts in controls, however, hepatic CREB phosphorylation remained elevated in STZ mice (Fig. 1*a*). Correspondingly, CRTC2 occupancy over gluconeogenic promoters was constitutively increased in STZ mice; and hepatic *PCK1* and *G6Pase* mRNA amounts were also up-regulated (Fig. 1, *b* and *c*). These results demonstrate the importance of circulating insulin in attenuating CREB and CRTC2 activities during feeding.

CRTC2 Activation Triggers Down-regulation of FOXO1—We wondered whether constitutive activation of the CREB pathway in liver is sufficient to stimulate the gluconeogenic program. Based on the ability for adeno-associated viruses (AAVs) to be stably maintained as extra-chromosomal plasmids in infected cells, we prepared adeno-associated virus serotype 8 containing a Flag epitope-tagged CRTC2 cDNA with Serine-Alanine substitutions at inhibitory (Ser-171, Ser-275) sites. Mice were injected retro-orbitally with adeno-associated viruses expressing $CRTC2S_{171,\ 275}A$ (denoted AAV.CRTC2AA) or control virus (AAV.Empty) and followed thereafter for 36 days. Total hepatic CRTC2 protein amounts were increased by 35% in hepatocytes from AAV.CRTC2AA mice relative to controls (Fig. 3*a*). We detected AAV-encoded CRTC2 only in liver, and not in quadriceps muscles, white adipose tissue, or brown adipose tissue (Fig. 2*a*).

To evaluate effects of the $CRTC2S_{171,275}AA$ protein on hepatic CREB activity, we used transgenic mice expressing a CRE-Luciferase reporter (17). CREB reporter activity was robustly increased in AAV.CRTC2AA mice relative to controls under fasting as well as refed conditions, when hepatic CREB activity is otherwise downregulated ($p < 0.05$, Fig. 2, *b* and *c*).

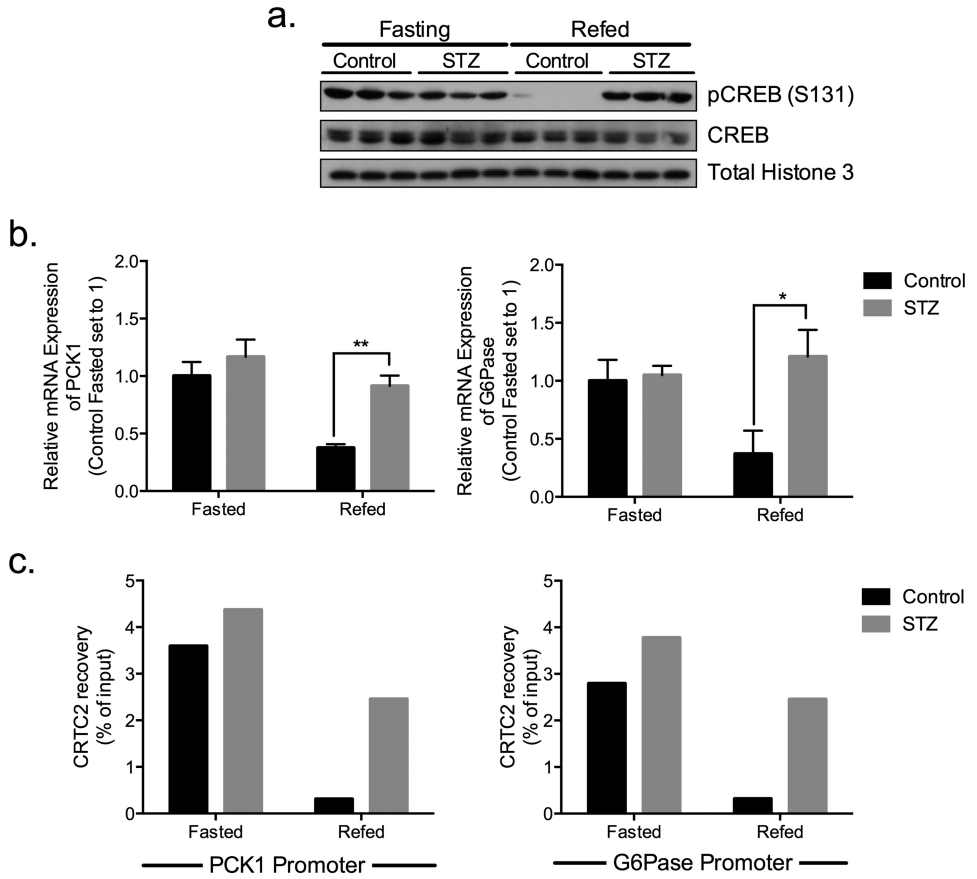

FIGURE 1. **Hepatic CREB and CRTC2 are active under fasting conditions.** *a*, immunoblot showing hepatic CREB (phosphorylated and total) under fasting and refed conditions in STZ treated and control mice. *b*, relative expression of *PCK1* and *G6Pase* in livers of fasted and refed STZ and control animals. Expression levels are normalized to L32 and expressed as fold change to control fasted mice, $n = 3$. *c*, ChIP assay of CRTC2 over *PCK1* and *G6Pase* promoters in livers from STZ or control mice under fasted and refed conditions; ChIP signals are normalized to total input.

Supporting the notion that CREB activity is increased in animals expressing constitutively active CRTC2, mRNA amounts for *G6Pase* expression were higher in AAV.CRTC2AA compared with controls under fasting conditions (Fig. 2*d*). mRNA amounts for *PCK1* and *G6Pase* were also up-regulated under fed conditions in AAV.CRTC2AA compared with control mice (Fig. 2*d*, demonstrating that induction of the CREB pathway in liver is indeed sufficient to stimulate the gluconeogenic program. As a result, feeding-associated suppression of *PCK1* expression was significantly blunted in livers of AAV.CRTC2AA mice (49% reduction) compared with controls (74% reduction; Fig. 2*d*).

We considered that overexpression of active CRTC2 could trigger compensatory down-regulation of the forkhead transcription factor FOXO1. Indeed, amounts of Ser-256 phosphorylated and therefore inactive FOXO1 were substantially increased in livers of *ad libitum* fed AAV.CRTC2AA mice (Fig. 2*e*). Despite these increases, FOXO1 phosphorylation was not sufficient to block CREB/CRTC2 activities.

Constitutive Nuclear Localization of Phosphorylation-defective CRTC2—In keeping with results in liver, CRTC2 mRNA amounts were increased nearly 2-fold in AAV.CRTC2AA hepatocytes (Fig. 3*a*). Under basal conditions, protein amounts for dephosphorylated (active; lower band on immunoblot) CRTC2 were increased by 67% in AAV.CRTC2AA compared with control (Fig. 3*a*).

CRTC2 contains a number of phosphorylation sites in addition to Ser-171 and -275 that also contribute to its mobility (8, 10, 23). We performed immuno-cytochemical studies to visualize differences in nuclear accumulation between control and CRTC2AA expressing cells. Endogenous CRTC2 was primarily localized to the cytoplasm in the basal state; it shuttled to the nucleus in response to glucagon. By contrast, overexpressed CRTC2AA appeared nuclear under both basal and glucagon-stimulated conditions (Fig. 3*b*). These results suggest that AAV-encoded CRTC2AA is primarily expressed in hepatocytes, where it is constitutively nuclear-localized. Indeed, mRNA amounts for gluconeogenic genes (*PCK1* and *G6Pase*) were up-regulated under basal conditions in hepatocytes from AAV-CRTC2AA mice. Exposure to glucagon further augmented *PCK1* ($p = 0.05$) and *G6Pase* ($p = 0.058$) expression to a greater extent in AAV.CRTC2AA hepatocytes compared with controls (Fig. 3*c*).

Altered Glucose Set Point in Mice Expressing Constitutively Active CRTC2—Having seen that gluconeogenic gene expression is increased in isolated hepatocytes as well as livers of mice expressing the phosphorylation-defective CRTC2 polypeptide, we examined whether circulating blood glucose concentrations are correspondingly altered. Supporting this notion, AAV.CRTC2AA expressing mice had higher fasting blood glucose relative to control animals, under both short-term and overnight fasting conditions over a 5-week period (Fig. 4, *a* and

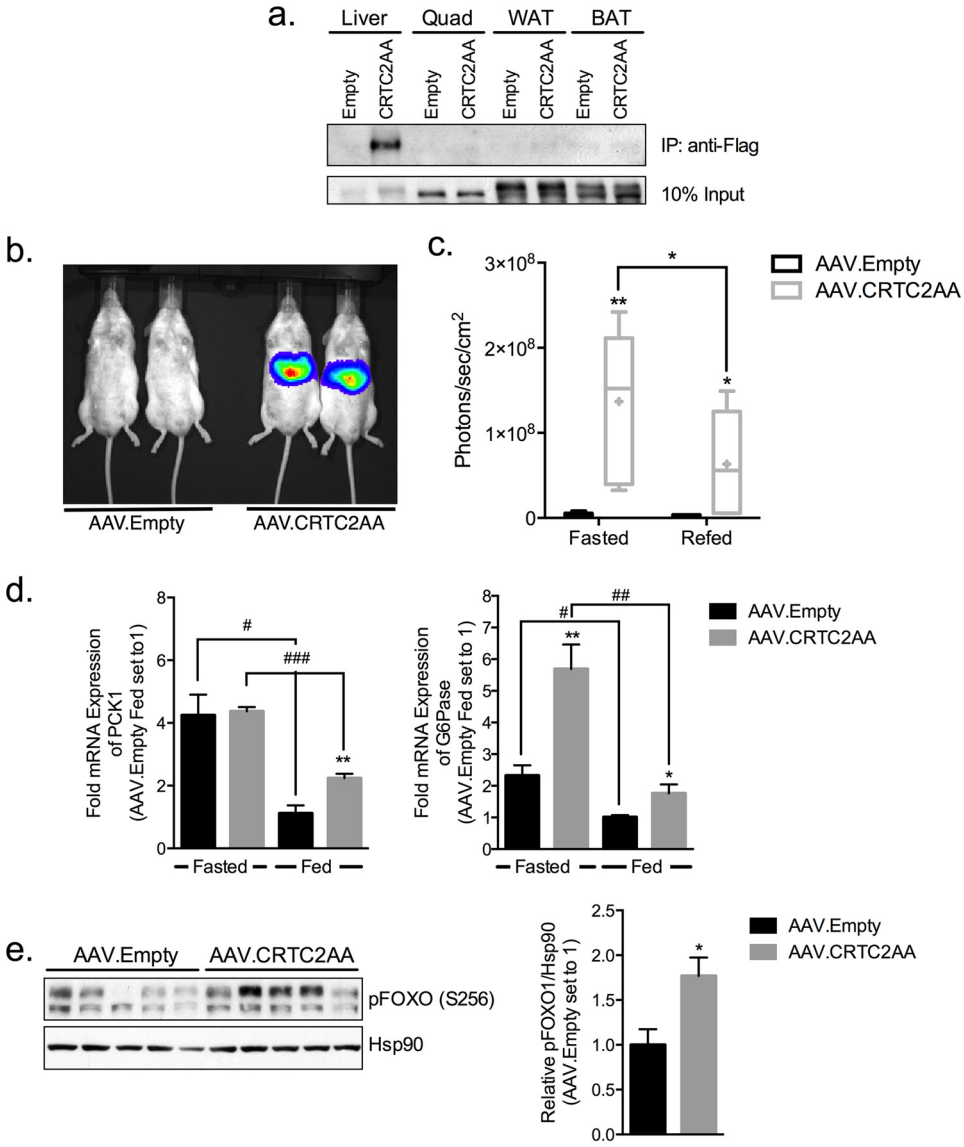

FIGURE 2. **Modest overexpression of a phosphorylation-defective CRTC2 polypeptide in liver stimulates gluconeogenic gene expression.** *a*, immunoblot showing CRTC2 protein amounts recovered from extracts of different tissues immunoprecipitation of FLAG epitope. Tissues were collected from mice infected with AAV.Empty or AAV.CRTC2AA (FLAG-tagged) viruses. *b*, representative live image of CRE-Luciferase reporter mice infected with AAV.Empty or AAV.CRTC2AA after 3 h of refeeding. *c*, quantification of hepatic CRE-luciferase expression in mice fasted overnight and refed for 3 h. Bars indicate upper and lower quartiles, + indicates mean, and error bars indicate minimum and maximum values, $n = 5–6$. *d*, relative expression of *PCK1* and *G6Pase* genes in livers of fasted and fed mice infected with AAV.Empty or AAV.CRTC2AA virus. Expression levels are normalized to *L32* and expressed as fold change to fed AAV. Empty mice (set to 1), $n = 5$. (*, $p < 0.05$; **, $p < 0.005$; ***, $p < 0.0005$ compared with AAV.Empty mice; #, $p < 0.05$; ##, $p < 0.005$; ###, $p < 0.0005$ compared with fasted/fed of same viral infection; data shown as mean ± S.E.). *e*, phospho-FOXO1 levels of in livers of fed animals 36 days post viral infection, quantification of blots shown to right. Biological replicates shown.

b). Notably, *ad libitum* fed blood glucose concentrations were also increased in AAV.CRTC2AA mice (Fig. 4*b*).

To determine whether these differences were due to increases in hepatic gluconeogenesis, we performed a pyruvate tolerance test. Although glucose output from pyruvate was increased in the AAV.CRTC2AA animals, this difference appears to reflect primarily an increase in fasting blood glucose levels, rather than a change in hepatic gluconeogenesis (Fig. 4*c*).

Glucose clearance appeared comparable between AAV.CRTC2AA and control mice by intraperitoneal glucose tolerance testing. In keeping with results from pyruvate tolerance testing, the incremental area under the curve was comparable between both groups suggesting that the differences in circulating glucose concentration is primarily driven by the initial elevation in fasting blood glucose levels (Fig. 4*d*). Indeed, AAV.CRTC2AA mice had a persistent and fixed elevation in blood glucose levels by continuous glucose monitoring throughout an entire light-dark cycle (Fig. 4*e*), pointing to a change in the set point for circulating glucose concentrations.

Hepatic Insulin Resistance and Steatosis in Mice Expressing Constitutively Active CRTC2—We performed insulin tolerance testing to determine whether the elevations in fed and fasted glucose levels in AAV.CRTC2AA mice were associated with insulin resistance. Following insulin administration, blood glucose concentrations decreased in control animals but they remained elevated in AAV.CRTC2AA mice, demon-

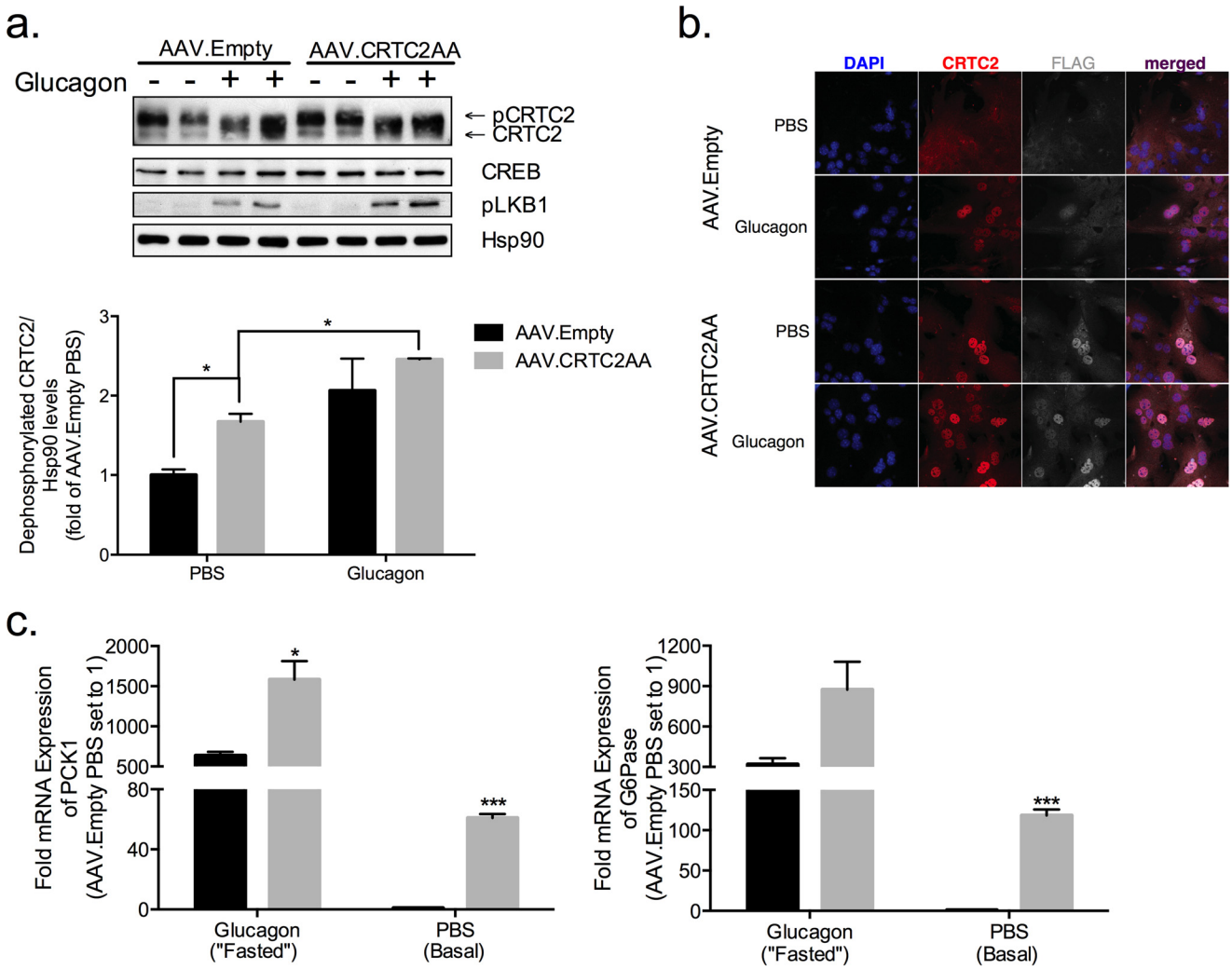

FIGURE 3. **Effect of phosphorylation-defective CRTC2 on gluconeogenic gene expression in isolated hepatocytes.** *a*, immunoblot of hepatocytes isolated from mice infected with AAV.Empty or AAV.CRTC2AA viruses. Cells were exposed to glucagon (100 nM) or PBS for 1 h. Amounts of dephosphorylated CRTC2 quantified below. (*, $p < 0.05$; data shown as mean ± S.E.) *b*, immunofluorescence images of hepatocytes isolated from mice infected with AAV.Empty or AAV.CRTC2AA (as in *a*). *c*, effect of glucagon or PBS (1 h) on gluconeogenic gene expression in hepatocytes isolated from mice previously infected with AAV. Empty or AAV.CRTC2AA. All expression values are normalized to *L32* and then expressed as fold change where hepatocytes from AAV. Empty mice treated with PBS are set to 1, $n = 3$. (*, $p < 0.05$; ***, $p < 0.0005$ compared with AAV. Empty of same treatment; data shown as mean ± S.E.)

strating that AAV.CRTC2AA mice are indeed insulin resistant (Fig. 5*a*).

To determine if the observed increase in insulin resistance is also transmitted to peripheral tissues (muscle and fat), we measured effects of insulin on AKT phosphorylation in epididymal white adipose tissue (WAT) and quadriceps muscles.

Phospho(Ser-473)AKT amounts appeared comparable between control and AAV.CRTC2AA mice under basal conditions and following insulin injection (Fig. 5*b*), indicating that the effects of CRTC2AA are likely confined to the liver. In keeping with the presence of hepatic insulin resistance, CRTC2AA mice had morphological evidence of hepatic steatosis (Fig. 5*c*). Hepatic triglycerides also appeared higher under under *ad libitum* fed conditions, although they did not reach the level of statistical significance ($p = 0.06$, Fig. 5*d*).

Hepatic insulin resistance is often associated with increased serum insulin levels under *ad libitum* conditions (Fig. 6*a*) and compensatory increases in islet cell mass. Indeed, β-cell area was increased 36% in AAV.CRTC2AA mice, whereas α-cell area was unchanged (Fig. 6, *b* and *c*). This increase was associated with an overall increase in islet area, and was due to the increase in islet cell number rather than cell size (Fig. 6*d*). Collectively, these results indicate that constitutive activation of the CREB pathway in liver is sufficient to promote insulin resistance and compensatory islet hyperplasia.

Discussion

Insulin resistance is a major risk factor for the development of type 2 diabetes, which is characterized by an inability for insulin to promote glucose uptake into muscle and to inhibit glucose production by the liver. Hepatic glucose output is elevated in type 2 diabetes, where it contributes to a number of complications including heart disease and peripheral neuropathy. We found that persistent activation of the CREB pathway in liver promotes hepatic steatosis and stimulates constitutive increases in blood glucose concentrations.

Hepatic expression of AAV-encoded CRTC2AA triggered substantial increases in the activity of a hepatic CREB reporter

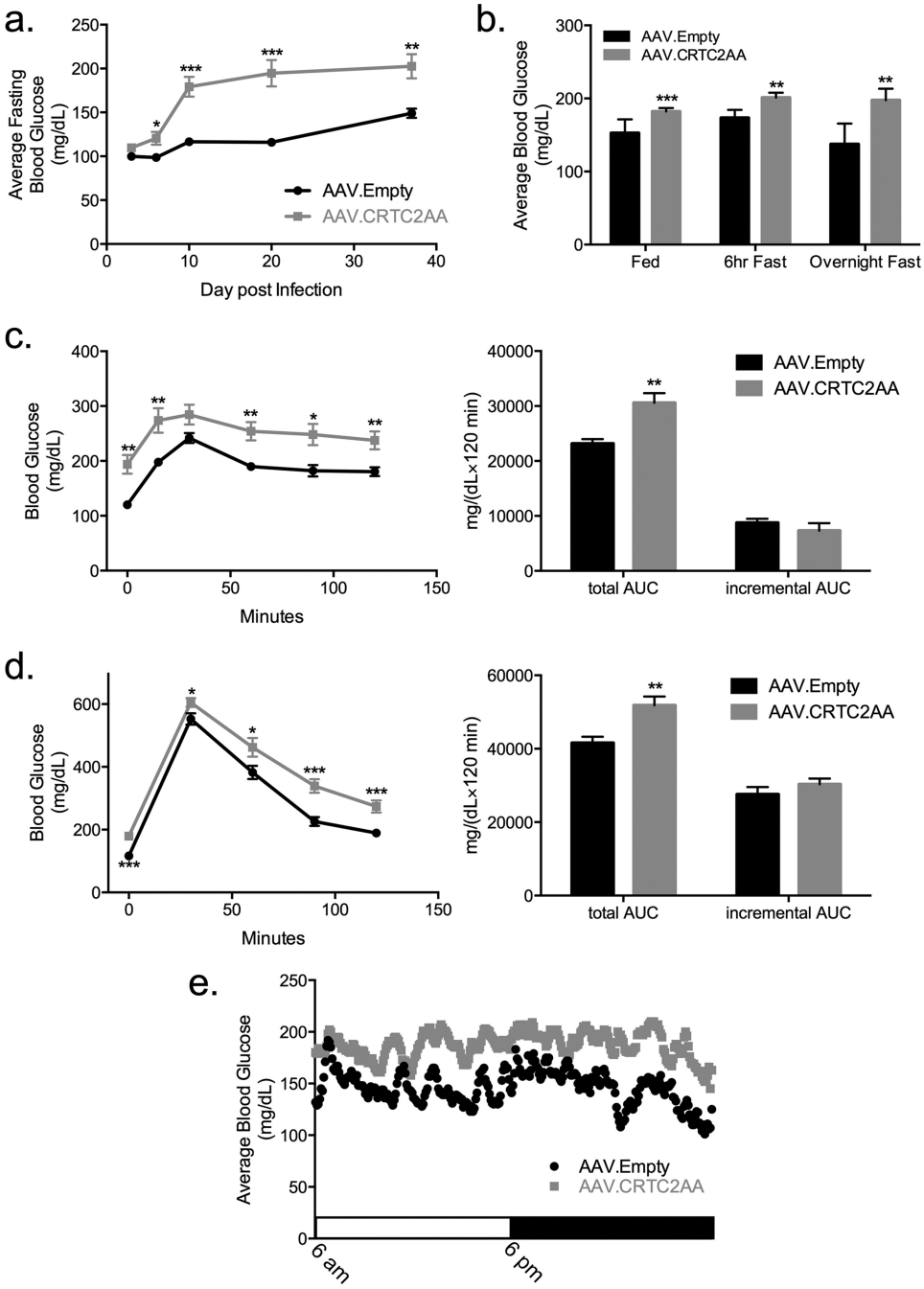

FIGURE 4. **Chronic activation of the CREB pathway in liver increases fasting blood glucose concentrations.** *a*, average overnight fasting blood glucose levels of mice infected with AAV.Empty or AAV.CRTC2AA over a 37-day period, $n = 10$. *b*, average blood glucose levels during ad-lib and fasting conditions; day 17–30, $n = 10–20$. *c*, pyruvate tolerance test on day 20 post virus injection, 2 g sodium pyruvate/kg mouse, $n = 7$. Right hand side of the figure shows calculated total area under the curve and incremental area under the curve. *d*, intraperitoneal glucose tolerance test on day 10 following viral infection, 1 g glucose/kg mouse, $n = 10$. *Right*, calculated total and incremental area under the curve. *e*, continuous glucose monitoring over a 24 h light/dark cycle with free access to food and water; $n = 2$ per group, 2 days of monitoring; average values shown. (*, $p < 0.05$; **, $p < 0.005$; ***, $p < 0.0005$ compared with AAV.Empty mice; data shown as mean ± S.E.).

that contains eight tandem CREB binding sites (17). By contrast, effects of CRTC2AA on gluconeogenic gene expression were more modest, likely reflecting in part compensatory increases in the AKT-mediated phosphorylation and inactivation of the forkhead transcription factor FOXO1 (Fig. 2). Hepatic expression of activated CRTC2 had no appreciable effect in other tissues, indicating that CREB/CRTC2 signaling primarily modulates hepatic insulin resistance.

Studies with STZ diabetic mice support an important role for insulin in attenuating CREB/CRTC activity during feeding. CRTC2 occupancy over gluconeogenic genes was increased in STZ diabetic mice primarily during feeding, when CRTC2 activity is otherwise down-regulated in response to insulin (21).

The chronic increases in CRTC2 activity and in gluconeogenic gene expression led to persistent elevations in fasting as

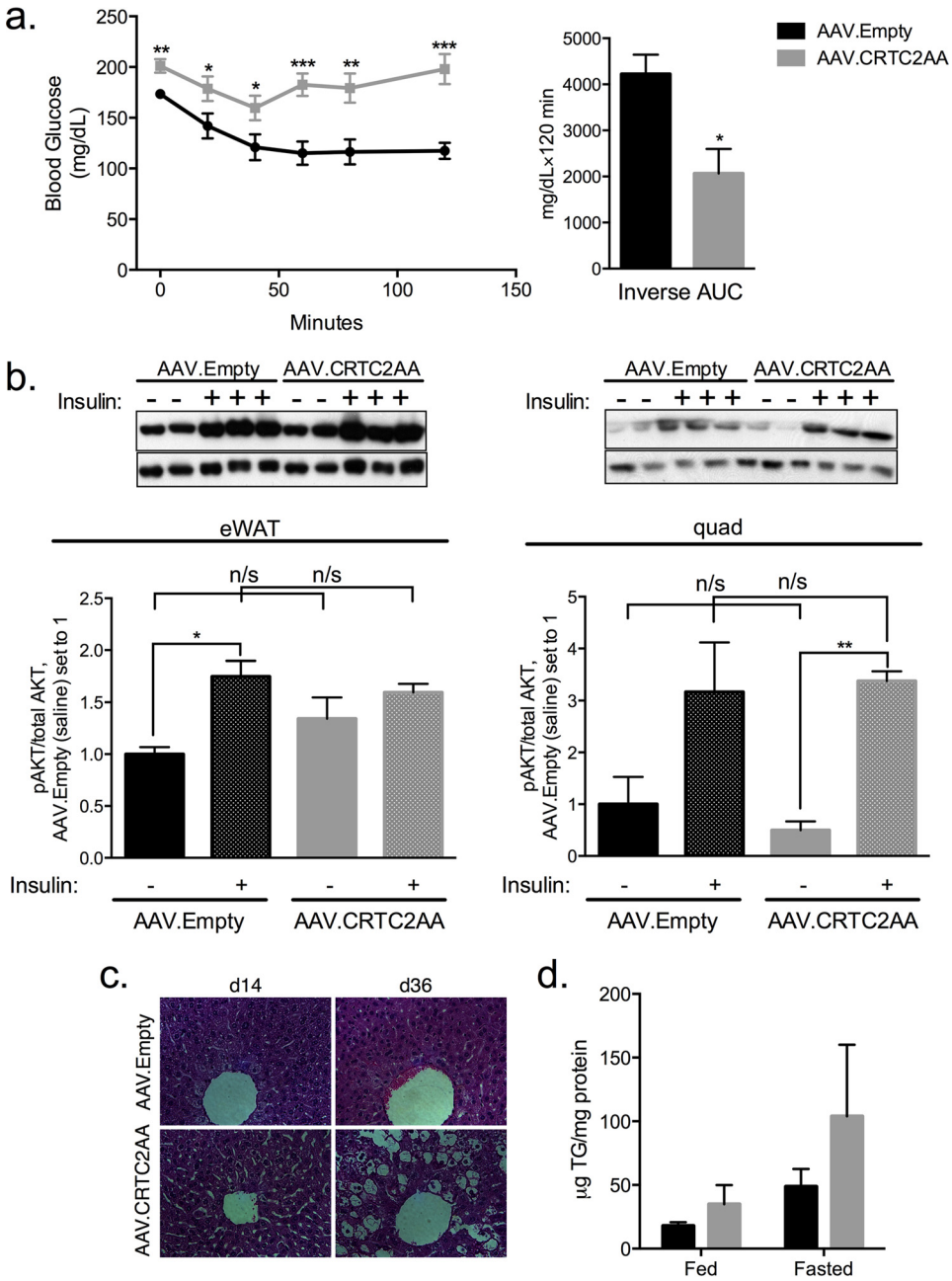

FIGURE 5. **Expression of phosphorylation-defective CRTC2 increases hepatic insulin resistance and steatosis.** *a*, insulin tolerance test on day 7 after viral infection, 1 unit insulin/kg mouse, $n = 8$. *Right*, calculated inverse area under the curve. *b*, epididymal WAT (*left*) and quad muscles (*right*) tissues probed for phospho- and total AKT 10 min post IP injection of saline or insulin (1 unit/kg mouse). Quantification is shown below the blots. *c*, H&E sections of livers from mice on day 14 and 36 post viral infection. *d*, liver triglycerides, day 36 post viral injection, standardized to mg total protein, $n = 5$. (*, $p < 0.05$; **, $p < 0.005$; ***, $p < 0.0005$ compared with AAV.Empty mice; data shown as mean ± S.E.).

well as *ad libitum* fed blood glucose levels. These observations indicate that the increase in gluconeogenesis is not suppressible and thus the baseline blood glucose of these animals has been "reset" to a higher level. Indeed, in continuous glucose monitoring studies, AAV.CRTC2AA mice had elevated blood glucose concentrations throughout the day/night cycle. As a result, mice expressing CRTC2AA are more insulin resistant due in part to the increase in hepatic gluconeogenesis. No direct measure of insulin resistance in liver was performed in our study, however; future work should confirm the apparent effects of CRTC2AA on hepatic glucose output.

Despite the presence of hepatic insulin resistance, the insulin response to the glucose challenge is appropriate to dispose of the glucose load at the same rate as in the control mice. This increase in the insulin response is consistent with the increase in β-cell area observed, which appears to be secondary to the hepatic insulin resistance.

The increase in islet area in AAV.CRTC2AA mice, which occurs due to hyperplasia rather than hypertrophy, appears to be limited to β cells and likely includes an increase in β-cell proliferation. Several mechanisms could underlie the expansion of β-cells in this setting. First, β-cell replication can be

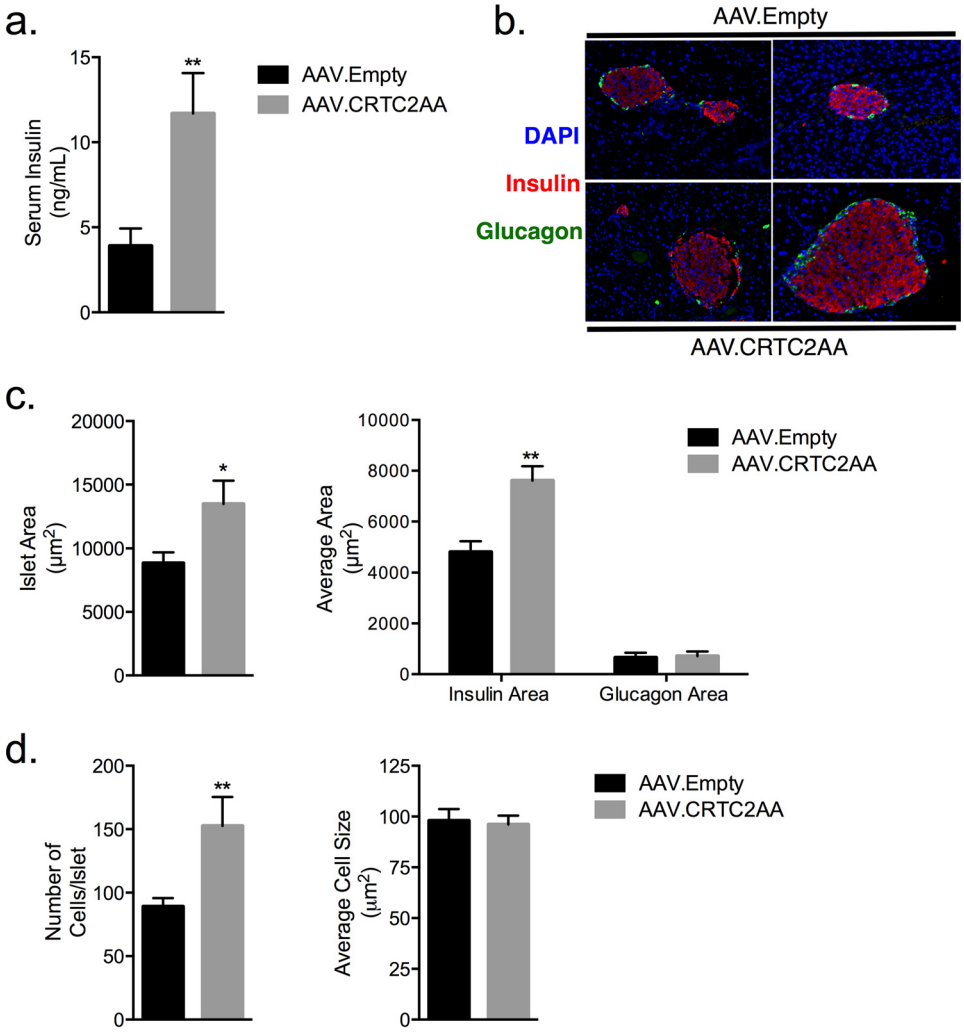

FIGURE 6. **Compensatory islet hyperplasia and hyperinsulinemia in mice expressing phosphorylation-defective CRTC2.** *a*, serum insulin levels of *ad-lib* mice, $n = 5$. *b*, representative IF images of islets of mice, day 36 post viral infection. *c*, quantification of total islet area (*left*), and insulin and glucagon area (*right*) of islets from day 36 post viral infection, $n = 5$ mice, with an average of 17 islets/animal. *d*, quantification of total cell numbers and size of islets from day 36 post viral infection. (*, $p < 0.05$; **, $p < 0.005$ compared with AAV.Empty mice; data shown as mean ± S.E.)

driven by increased secretory demand placed upon the islet by dietary-fat-induced obesity and insulin resistance or chronic, mild hyperglycemia (24, 25). Additionally, secreted factors such as hepatocyte growth factor or glucagon-like peptide-1 can induce β-cell replication (26–28). It is also possible that the constitutively active expression of CRTC2 in the liver promotes transcription of a liver derived factor, which then promotes β-cell hyperplasia, such as that described by El Ouaamari *et al.* in 2013 (29). Future studies should provide insight into this process.

We found that a persistent increase in CREB activity for a period of 5 weeks is sufficient to produce hepatic insulin resistance, leading to fasting hyperglycemia. Our studies also reveal that hepatic CREB signaling determines the homeostatic set point for plasma glucose concentrations. This persistent hyperglycemia was associated with a compensatory increase in β-cell area and an elevation of circulating insulin levels, thus preventing dramatic increases in fasting and post-prandial glucose. Future studies should reveal whether increases in circulating insulin concentrations promote fat accumulation in the liver, which is associated with insulin resistance (30–34).

Author Contributions—M. F. H. designed the study and performed the experiments, analyzed data, and wrote the manuscript. K. R. performed STZ studies and ChIP analysis of CRTC2 occupancy. S. M. performed the immunofluorescence of isolated hepatocytes and reviewed/edited the manuscript. M. O. H. assisted with the CGMS and reviewed/edited the manuscript. R. L. H. and S. E. K. analyzed and interpreted the data on islet morphology, and reviewed/edited the manuscript. M. M. designed the study, the experiments, analyzed data, and reviewed/edited the manuscript. All authors reviewed the results and approved the final version of the manuscript.

Acknowledgments—We thank Emilie Blanchet and Naomi Philips for technical help with the work reported in this manuscript.

References

1. Barthel, A., and Schmoll, D. (2003) Novel concepts in insulin regulation of hepatic gluconeogenesis. *Am. J. Physiol. Endocrinol Metab.* **285,** E685-E692
2. Samuel, V. T., and Shulman, G. I. (2012) Mechanisms for Insulin Resistance: Common Threads and Missing Links. *Cell* **148,** 852–871
3. Saltiel, A. R., and Kahn, C. R. (2001) Insulin signalling and the regulation of glucose and lipid metabolism. *Nature* **414,** 799–806

4. Biddinger, S. B., and Kahn, C. R. (2006) FROM MICE TO MEN: Insights into the Insulin Resistance Syndromes. *Annu. Rev. Physiol.* **68,** 123–158
5. Herzig, S., Long, F., Jhala, U. S., Hedrick, S., Quinn, R., Bauer, A., Rudolph, D., Schutz, G., Yoon, C., Puigserver, P., Spiegelman, B. M., and Montminy, M. R. (2001) CREB regulates hepatic gluconeogenesis through the coactivator PGC-1. *Nature* **413,** 179–183
6. Hagiwara, M., Brindle, P. K., Harootunian, A., Armstrong, R., Rivier, J., Vale, W., Tsien, R., and Montminy, M. R. (1993) Coupling of hormonal stimulation and transcription via the cyclic AMP-responsive factor CREB is rate limited by nuclear entry of protein kinase A. *Mol. Cell Biol.* **13,** 4852–4859
7. Chrivia, J. C., Kwok, R. P., Lamb, N., Hagiwara, M., Montminy, M. R., and Goodman, R. H. (1993) Phosphorylated CREB binds specifically to the nuclear protein CBP. *Nature* **365,** 855–859
8. Screaton, R. A., Conkright, M. D., Katoh, Y., Best, J. L., Canettieri, G., Jeffries, S., Guzman, E., Niessen, S., Yates, J. R., 3rd, Takemori, H., Okamoto, M., and Montminy, M. R. (2004) The CREB coactivator TORC2 functions as a calcium- and cAMP-sensitive coincidence detector. *Cell* **119,** 61–74
9. Koo, S.-H., Flechner, L., Qi, L., Zhang, X., Screaton, R. A., Jeffries, S., Hedrick, S., Xu, W., Boussouar, F., Brindle, P. K., Takemori, H., and Montminy, M. R. (2005) The CREB coactivator TORC2 is a key regulator of fasting glucose metabolism. *Nature* **437,** 1109–1111
10. Dentin, R., Hedrick, S., Xie, J., Yates, J., 3rd, and Montminy, M. R. (2008) Hepatic Glucose Sensing via the CREB Coactivator CRTC2. *Science* **319,** 1402–1405
11. Wang, X. L., Suzuki, R., Lee, K., Tran, T., Gunton, J. E., Saha, A. K., Patti, M.-E., Goldfine, A. B., Ruderman, N. B., Gonzalez, F. J., and Kahn, C. R. (2009) Ablation of ARNT/HIF1β; in Liver Alters Gluconeogenesis, Lipogenic Gene Expression, and Serum Ketones. *Cell Metab.* **9,** 428–439
12. Wang, Y., Inoue, H., Ravnskjaer, K., Viste, K., Miller, N., Liu, Y., Hedrick, S., Vera, L., and Montminy, M. R. (2010) Targeted disruption of the CREB coactivator Crtc2 increases insulin sensitivity. *Proc. Natl. Acad. Sci. U.S.A.* **107,** 3087–3092
13. Luo, Q., Luo, Q., Viste, K., Viste, K., Urday-Zaa, J. C., Urday-Zaa, J. C., Kumar, G. S., Tsai, W.-W., Talai, A., Mayo, K. E., Montminy, M. R., and Radhakrishnan, I. (2012) Mechanism of CREB recognition and coactivation by the CREB-regulated transcriptional coactivator CRTC2. *Proc. Natl. Acad. Sci. U.S.A.* **109,** 20865–20870
14. Saberi, M., Bjelica, D., Schenk, S., Imamura, T., Bandyopadhyay, G. K., Li, P., Jadhar, V., Vargeese, C., Wang, W., Bowman, K., Zhang, Y., Polisky, B., and Olefsky, J. M. (2009) Novel liver-specific TORC2 siRNA corrects hyperglycemia in rodent models of type 2 diabetes. *AJP: Endocrinology and Metabolism.* **297,** E1137–E1146
15. Le Lay, J., Tuteja, G., White, P., Dhir, R., Ahima, R. S., and Kaestner, K. H. (2009) CRTC2 (TORC2) Contributes to the Transcriptional Response to Fasting in the Liver but Is Not Required for the Maintenance of Glucose Homeostasis. *Cell Metab.* **10,** 55–62
16. Ravnskjaer, K., Hogan, M. F., Lackey, D., Tora, L., Dent, S. Y. R., Olefsky, J. M., and Montminy, M. R. (2013) Glucagon regulates gluconeogenesis through KAT2B- and WDR5-mediated epigenetic effects. *J. Clin. Invest.* **123,** 4318–4328
17. Song, Y., Altarejos, J. Y., Goodarzi, M. O., Inoue, H., Guo, X., Berdeaux, R., Kim, J.-H., Goode, J., Igata, M., Paz, J. C., Hogan, M. F., Singh, P. K., Goebel, N., Vera, L., Miller, N., Cui, J., Jones, M. R., CHARGE Consortium, GIANT Consortium, Chen, Y.-D. I., Taylor, K. D., Hsueh, W. A., Rotter, J. I., and Montminy, M. R. (2010) CRTC3 links catecholamine signalling to energy balance. *Nature* **468,** 933–939
18. Miller, R. A., Chu, Q., Le Lay, J., Scherer, P. E., Ahima, R. S., Kaestner, K. H., Foretz, M., Viollet, B., and Birnbaum, M. J. (2011) Adiponectin suppresses gluconeogenic gene expression in mouse hepatocytes independent of LKB1-AMPK signaling. *J. Clin. Invest.* **121,** 2518–2528
19. Lu, M., Wan, M., Leavens, K. F., Chu, Q., Monks, B. R., Fernandez, S., Ahima, R. S., Ueki, K., Kahn, C. R., and Birnbaum, M. J. (2012) Insulin regulates liver metabolism in vivo in the absence of hepatic Akt and Foxo1. *Nat. Med.* **18,** 388–395
20. van der Meulen, T., Donaldson, C. J., Cáceres, E., Hunter, A. E., Cowing-Zitron, C., Pound, L. D., Adams, M. W., Zembrzycki, A., Grove, K. L., and Huising, M. O. (2015) Urocortin3 mediates somatostatin-dependent negative feedback control of insulin secretion. *Nat. Med.* 10.1038/nm.3872
21. Dentin, R., Liu, Y., Koo, S.-H., Hedrick, S., Vargas, T., Heredia, J. E., Yates, J. R., 3rd, and Montminy, M. R. (2007) Insulin modulates gluconeogenesis by inhibition of the coactivator TORC2. *Nature* **449,** 366–369
22. Hull, R. L., Andrikopoulos, S., Verchere, C. B., Vidal, J., Wang, F., Cnop, M., Prigeon, R. L., and Kahn, S. E. (2003) Increased dietary fat promotes islet amyloid formation and β-cell secretory dysfunction in a transgenic mouse model of islet amyloid. *Diabetes* **52,** 372–379
23. Uebi, T., Tamura, M., Horike, N., Hashimoto, Y. K., and Takemori, H. (2010) Phosphorylation of the CREB-specific coactivator TORC2 at Ser^{307} regulates its intracellular localization in COS-7 cells and in the mouse liver. *Am. J. Physiol. Endocrinol Metab.* **299,** E413-E425
24. Hull, R. L., Kodama, K., Utzschneider, K. M., Carr, D. B., Prigeon, R. L., and Kahn, S. E. (2005) Dietary-fat-induced obesity in mice results in beta cell hyperplasia but not increased insulin release: evidence for specificity of impaired beta cell adaptation. *Diabetologia.* **48,** 1350–1358
25. Alonso, L. C., Yokoe, T., Zhang, P., Scott, D. K., Kim, S. K., O'Donnell, C. P., and Garcia-Ocaña, A. (2007) Glucose Infusion in Mice: A New Model to Induce β-Cell Replication. *Diabetes* **56,** 1792–1801
26. Nielsen, J. H., Svensson, C., Galsgaard, E. D., Møldrup, A., and Billestrup, N. (1999) Beta cell proliferation and growth factors. *J. Mol. Med.* **77,** 62–66
27. Garcia-Ocaña, A., Takane, K. K., Syed, M. A., Philbrick, W. M., Vasavada, R. C., and Stewart, A. F. (2000) Hepatocyte growth factor overexpression in the islet of transgenic mice increases beta cell proliferation, enhances islet mass, and induces mild hypoglycemia. *J. Biol. Chem.* **275,** 1226–1232
28. Stoffers, D. A., Kieffer, T. J., Hussain, M. A., Drucker, D. J., Bonner-Weir, S., Habener, J. F., and Egan, J. M. (2000) Insulinotropic glucagon-like peptide 1 agonists stimulate expression of homeodomain protein IDX-1 and increase islet size in mouse pancreas. *Diabetes* **49,** 741–748
29. El Ouaamari, A., Kawamori, D., Dirice, E., Liew, C. W., Shadrach, J. L., Hu, J., Katsuta, H., Hollister-Lock, J., Qian, W.-J., Wagers, A. J., and Kulkarni, R. N. (2013) Liver-Derived Systemic Factors Drive β Cell Hyperplasiain Insulin-Resistant States. *Cell Reports* **3,** 401–410
30. Ryysy, L., Häkkinen, A.-M., Goto, T., Vehkavaara, S., Westerbacka, J., Halavaara, J., and Yki-Järvinen, H. (2000) Hepatic fat content and insulin action on free fatty acids and glucose metabolism rather than insulin absorption are associated with insulin requirements during insulin therapy in type 2 diabetic patients. *Diabetes* **49,** 749–758
31. Seppälä-Lindroos, A., Vehkavaara, S., Häkkinen, A.-M., Goto, T., Westerbacka, J., Sovijärvi, A., Halavaara, J., and Yki-Järvinen, H. (2002) Fat accumulation in the liver is associated with defects in insulin suppression of glucose production and serum free fatty acids independent of obesity in normal men. *J. Clin. Endocrinol. Metab.* **87,** 3023–3028
32. Qatanani, M., and Lazar, M. A. (2007) Mechanisms of obesity-associated insulin resistance: many choices on the menu. *Genes Dev.* **21,** 1443–1455
33. Hardy, O. T., Czech, M. P., and Corvera, S. (2012) What causes the insulin resistance underlying obesity? *Curr. Opin. Endocrinol. Diab. Obes.* **19,** 81–87
34. Nagle, C. A., Klett, E. L., and Coleman, R. A. (2009) Hepatic triacylglycerol accumulation and insulin resistance. *J. Lipid Res.* **50,** S74-S79